Table S1: Kcnq1 (KCNQ1, KvLQT1) mRNA detected with various methods in multiple tissues as reported in the literature.							
Citation	**Detection Method**	**Probe**	**Age**	**Tissue**		**Species**	**Sample**
				Detected	**Not Detected**		
Sanguinetti et al. 1996 (S1)	Northern blot	1.2 kb probe (both isoforms)	Adult	Heart, placenta, lung, kidney, pancreas	Brain, liver, skeletal muscle	Human	MTN Blot I (Clontech)
Choabe et al. 1997 (S2)	Northern blot	905 bp probe (both isoforms)	Adult	Heart, placenta, lung, kidney, pancreas, spleen, thymus prostate, testis, ovary, small intestine, colon, peripheral blood leukocyte	Brain, liver, skeletal muscle	Human	MTN Blot I and MTN Blot II (Clontech)
		122 bp probe (IsoA)	Adult	Heart, placenta, lung, kidney, pancreas, prostate, small intestine, colon, peripheral blood leukocyte	Brain, liver, skeletal muscle, spleen, thymus, testis, ovary	Human	MTN Blot I and MTN Blot II (Clontech)
Lee et al. 1997 (S3)	RT-PCR	Primer set with primer in exon 1a (IsoA)	Fetal	Heart, gut, trachea, lung, kidney, limb, intestine	Tongue, brain, testis	Human	fetal tissue (University of Washington)
		Primer set with primer in 5' UTR (IsoB)	Fetal	Heart	Gut, trachea, lung, tongue, kidney, brain, testis, limb, intestine	Human	fetal tissue (University of Washington)
Jiang et al.1998 (S4)	RT-PCR	5 pairs of primers spanning exons covering entire gene (both isoforms)	Adult (8 weeks)	Heart, liver, intestine, kidney, lung, tail, gonad, brain, skeletal muscle	N/A	Mouse	F1 cross female 129 x male CS and reciprocal cross
			E12.5	Heart, liver, intestine, tail, gonad, brain, limb bud,	N/A	Mouse	F1 cross female 129 x male CS and reciprocal cross
			E6.5	Whole embryo	N/A	Mouse	F1 cross female 129 x male CS and reciprocal cross
			Newborn	Heart, liver, intestine, kidney, lung, tail, gonad, brain	N/A	Mouse	F1 cross female 129 x male CS and reciprocal cross
Kubisch et al. 1999 (S5)	RT-PCR	Primers across exon boundary in C-terminus of coding seq (both isoforms)	Adult	Cochlea, vestibule, brain (>30 cycles)	Brain (30 cycles)	Mouse	Brain, Ear (cochlea and vestibule)

Table S1: Kcnq1 (KCNQ1, KvLQT1) mRNA detected with various methods in multiple tissues as reported in the literature. Cont'd

Citation	Detection Method	Probe	Age	Tissue		Species	Sample
				Detected	Not Detected		
Delombe et al. 2001 (S6)	In situ hybridization	789 bp probe for 3' UTR (both isoforms)	Adult (6 weeks)	Kidney, small intestine, skeletal muscle, pancreas, stomach, esophagus, lung, trachea, heart, liver, thymus	spleen	Mouse	FVB mice
		789 bp probe for 3' UTR (both isoforms)	E16.5-18.5	Pancreas, villus/mid-villus	N/A	Mouse	FVB mice
	RNA protection assay	446 bp probe in 3' UTR (both isoforms)	Adult	5 day exposure: kidney, stomach, heart, small intestine, lung 10 day exposure: skeletal muscle, liver, thymus	N/A	Mouse	FVB mice
	RT-PCR	Primer set in 3' UTR (both isoforms)	Adult	Gut, lung, liver, skeletal muscle, thymus, spleen, heart	N/A	Mouse	FVB mice
Luo et al. 2008 (S7)	Real-time RT-PCR	TaqMan Quantitative Assay (IsoA)	Adult (59-72 yrs)	Heart, brain, liver, kidney, lung, breast, pancreas, colon, skeletal muscle	N/A	Human	Tissue (Ambion)
		TaqMan Quantitative Assay (IsoB)	Adult (59-72 yrs)	Heart, brain, kidney, lung, breast, pancreas, colon	Liver, skeletal muscle	Human	Tissue (Ambion)

MTN - Multiple Tissue Northern; RT-PCR - Reverse Transcrtiption Polymerase Chain Reaction; CS - CAST/Ei mouse strain (*Mus musculus castaneus*); N/A - Not applicable; UTR - untranslated region; IsoA - Isoform A of KCNQ; FVB - Friend leukemia virus B (*Fv1b* allele) mouse strain

Table S2: Time domain indices of heart rate variability in individual *T311I/T311I* and *A340E/A340E* mice as compared to wildtype littermates.

Parameter	T311I/T311I #1	T311I/T311I #2	T311I wildtype #1	T311I wildtype #2	A340E/A340E #1	A340E/A340E #2	A340E wildtype #1	A340E wildtype #2
RR (ms)[1]	117.8	110.0	101.9	100.4	127.5	105.7	101.2	113.6
SDNN (ms)[2]	13.2	9.5	8.8	5.4	13.3	5.4	4.6	10.9
CV (%)[3]	11.20%	8.68%	8.64%	5.38%	10.41%	5.12%	4.50%	9.59%
pNN6 (%)[4]	37.3%	16.3%	13.7%	11.2%	40.6%	6.8%	2.7%	31.7%
rMSSD (ms)[5]	8.16	5.52	4.93	3.79	9.29	4.97	2.12	6.77

[1]RR = time between two consecutive R waves in an ECG

[2]SDNN = standard deviation of the normal RR intervals

[3]CV = coefficient of variation (= SDNN/mean RR interval)

[4]rMSSD = root mean square of successive differences between adjacent normal RR intervals

[5]pNN6 = percentage of those differences between adjacent normal RR intervals >6 ms

SUPPORTING ONLINE MATERIAL Goldman et al.

Supplemental Online Videos

Video S1: Spontaneous EEG seizure without clonic movements or other overt behavioral component in heterozygous T311I mutant. Upper two EEG traces are left and right temporal electrodes, respectively. Lower two traces are left and right parietal electrodes.

Video S2: Spontaneous clonic seizure in heterozygous A340E mutant with simultaneous EEG-ECG recording. Upper two EEG traces are left and right temporal electrodes, respectively. Lower two traces are left and right parietal electrodes.

Supplemental Figures

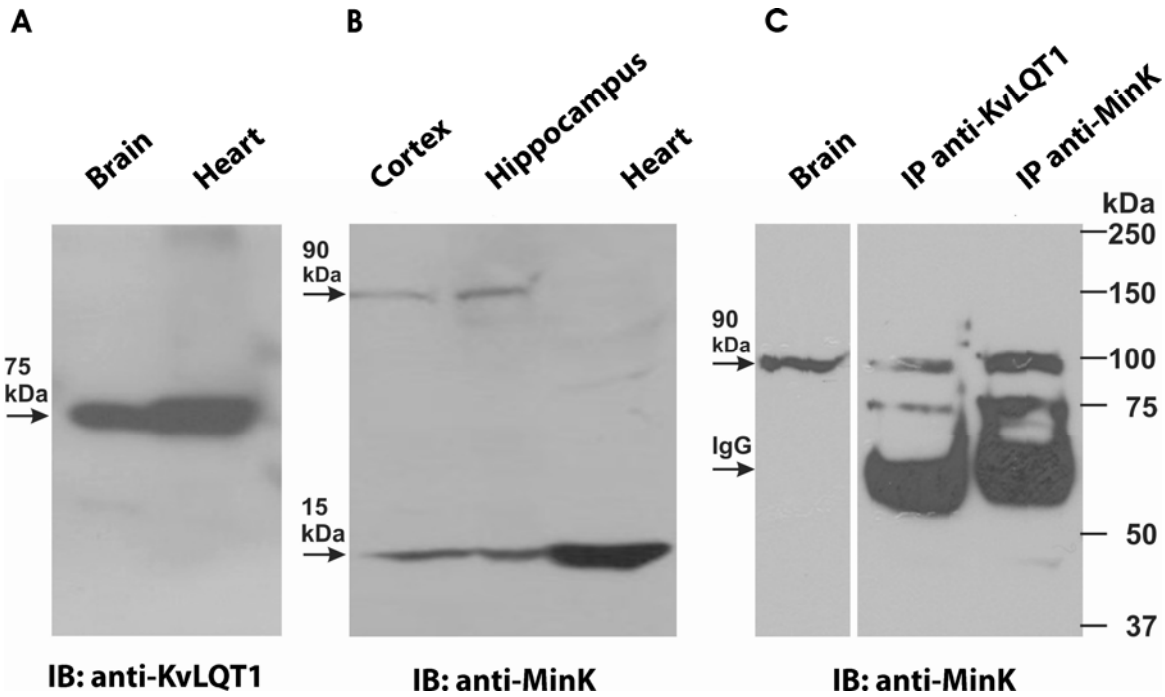

Figure S1: Full Gel Images for Western and Co-Immunoprecipitation Experiments
(A) Immunoreactive bands with apparent molecular weight of ~75 kDa corresponding to murine KvLQT1 pore-forming α-subunits were detected in protein lysates of mouse brain and heart by Western immunoblotting (IB) with the polyclonal antibody to KvLQT1.
(B) MinK protein subunits in the mouse cortex, hippocampus and heart. Immunoreactive bands with apparent molecular weight of ~15 kDa corresponding to murine MinK subunits were detected in protein lysates of mouse cortex, hippocampus and heart by Western immunoblotting with the polyclonal antibody to MinK. Immunoreactive bands at ~90 kDa were also detected in protein lysates of mouse whole brain, cortex and hippocampus.
(C) Immunoreactive bands at ~90 kDa were detected in co-immunoprecipitates (IP) of mouse whole brain with antibodies to KvLQT1 and MinK, followed by immunoblotting with the antibody to MinK. Western IB of brain with anti-MinK shows the ~90kDa band.

Figure S2: The pore of KCNQ1 channels is highly conserved.

Multiple alignment of protein sequences of KCNQ1 IsoA of selected vertebrates showing the conserved protein structure of the pore region. The black boxes indicate the conserved positions of the human T312I and A341E mutations. The grey boxes indicate the sole amino acid difference observed in the pore region of the frog (*X. laevis*) and zebrafish *(D. rerio*) channels. Full length protein sequences for both all channels were used in the multiple alignment. The multiple alignment was performed using the MUSCLE webserver (S9,S10).

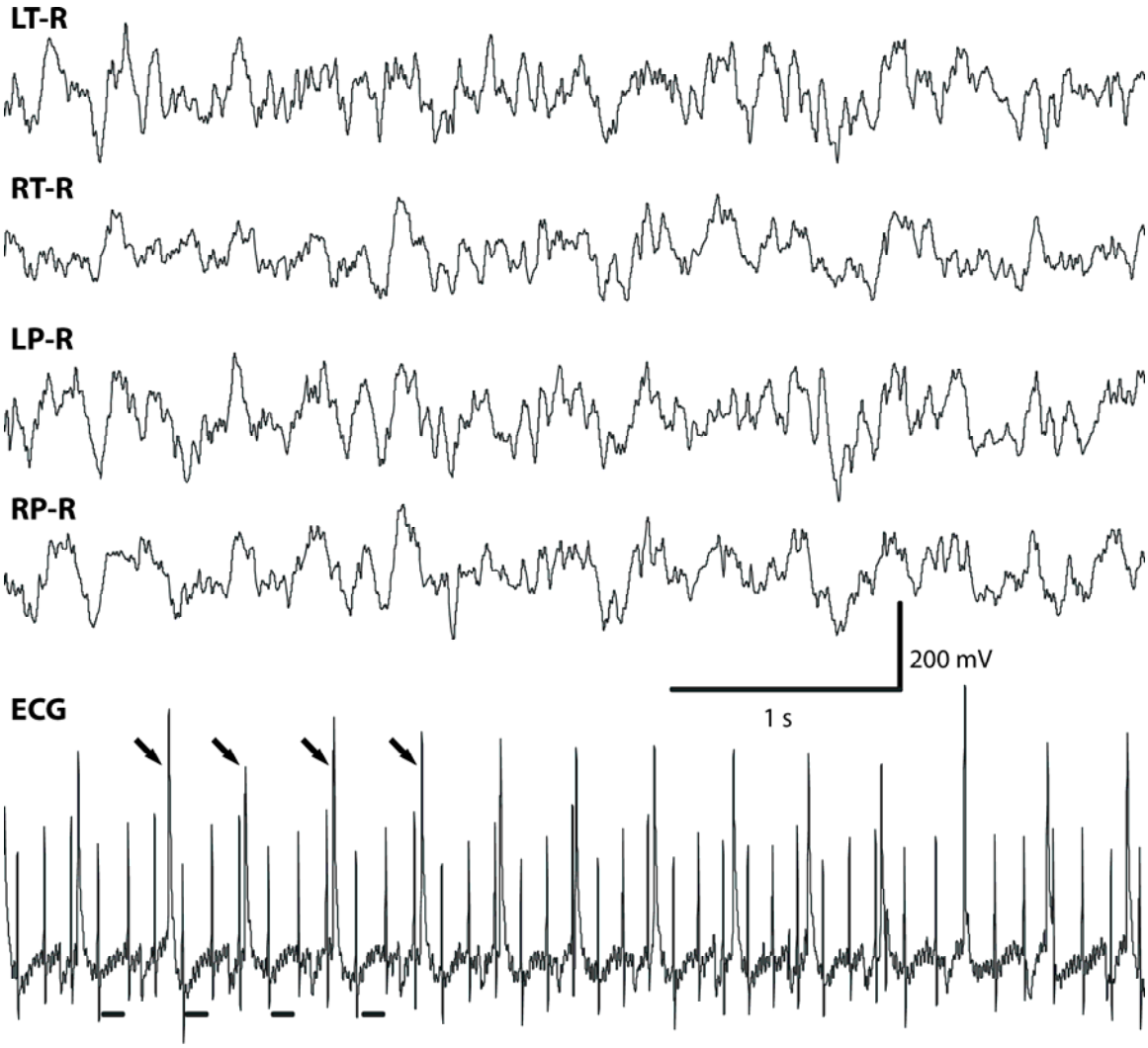

Figure S3: *T311I/T311I* mouse ECG showing atrial flutter with premature ventricular contractions. Baseline atrial flutter is marked with horizontal bar. The regularly occuring premature ventricular contractions are marked by arrows. Upper two EEG traces are left and right temporal electrodes, respectively. Lower two traces are left and right parietal electrodes.

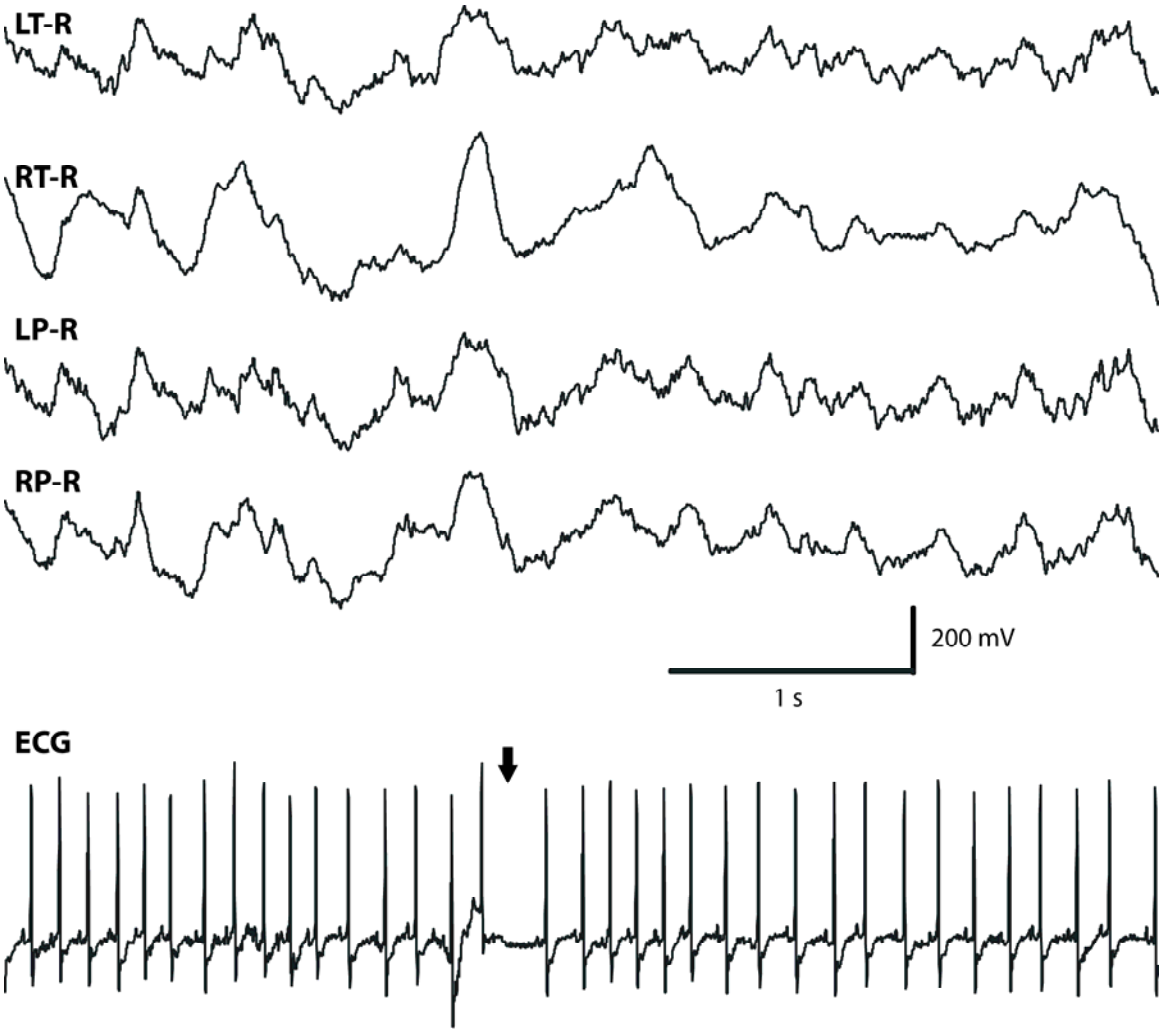

Figure S4: *T311I/T311I* mouse ECG showing a sinus pause. Isolated sinus pause (arrow) occured during a period of normal EEG activity. Upper two EEG traces are left and right temporal electrodes, respectively. Lower two traces are left and right parietal electrodes.

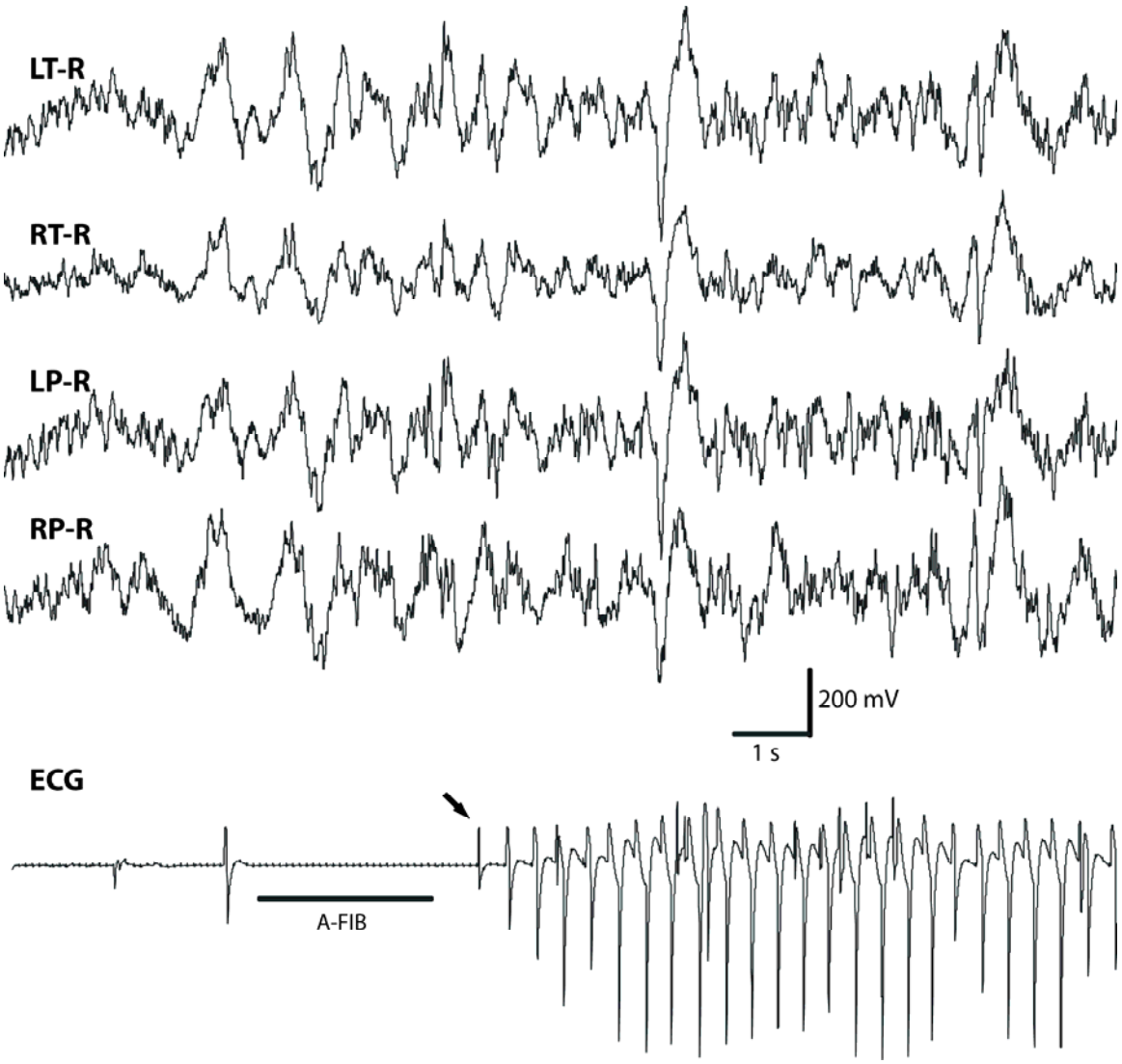

Figure S5: *A340E/A340E* mouse ECG showing atrial fibrillation with an idio-ventricular rhythm. Atrial fibrillation with AV block (underline) followed by an idio-ventricular rhythm (arrow). The event was associated with an episode of behavioral arrest. Upper two EEG traces are left and right temporal electrodes, respectively. Lower two traces are left and right parietal electrodes.

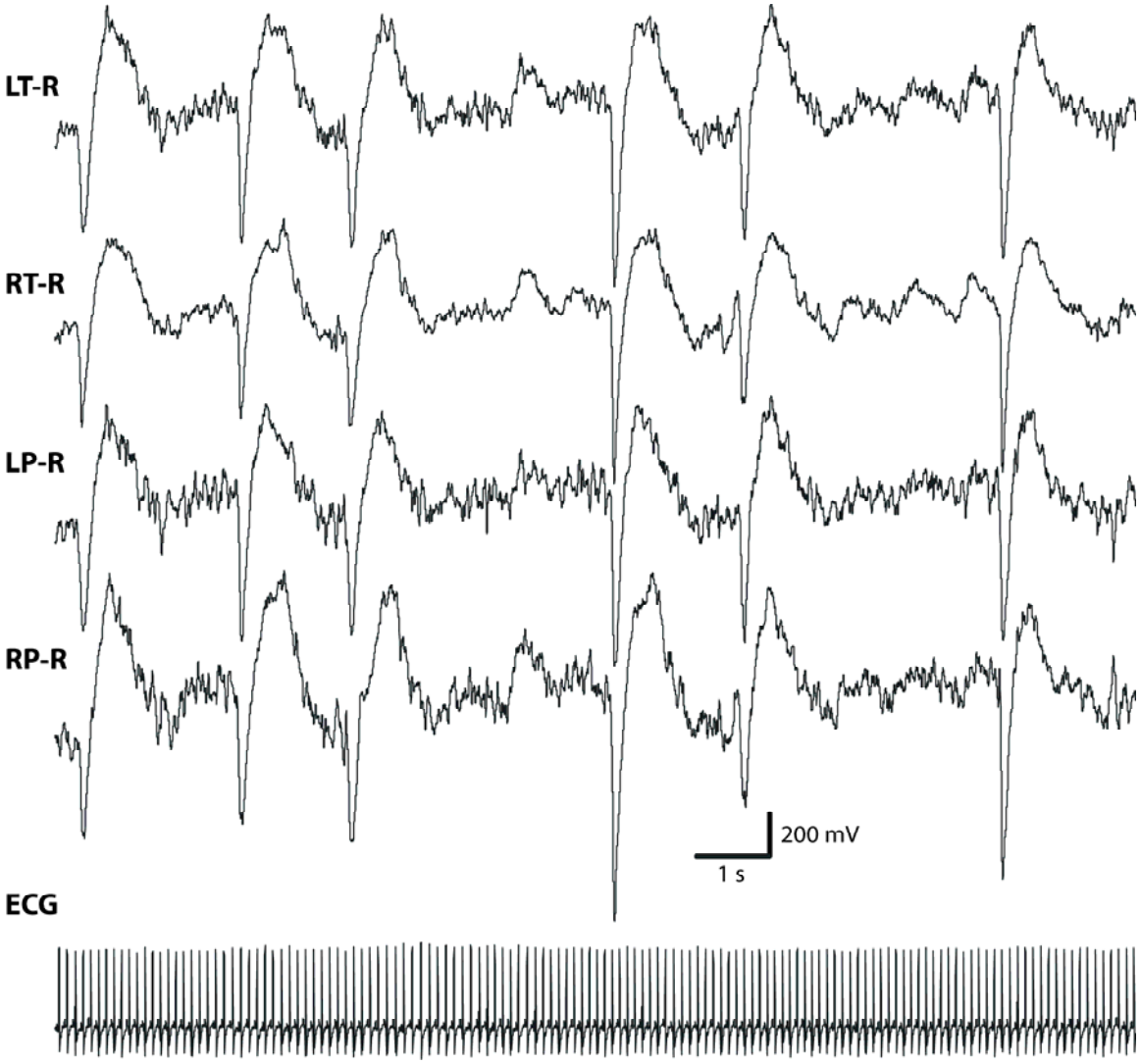

Figure S6: A340I/A340I mouse during seizure activity. Not all brain discharges trigger cardiac arrythmias. Upper two EEG traces are left and right temporal electrodes, respectively. Lower two traces are left and right parietal electrodes.

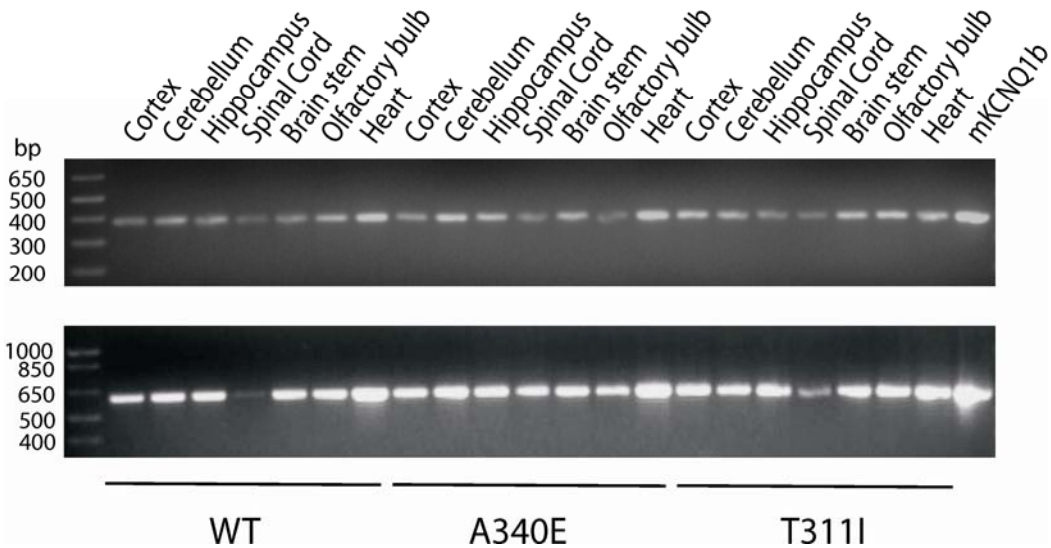

Figure S7: Functional channels containing the pore region encoded by exon 7 are expressed in both T311I and A340E mutant mice.

(Top) RT-PCR with primers designed to span the exon-exon boundaries of exons 5/6 (forward) and exons 7/8 (reverse). The expected 385 bp product was observed in *WT*, *A340E* and *T311I* mutant mice in all regions of the brain and heart.
(Bottom) RT-PCR with primers seated in the middle of exon 5 (forward) and exon 10 (reverse) resulted in the expected 582 bp product. Additional RT-PCR reactions for alternative splicing in the pore region were performed with mouse primer sequences (S8) and showed no PCR products.

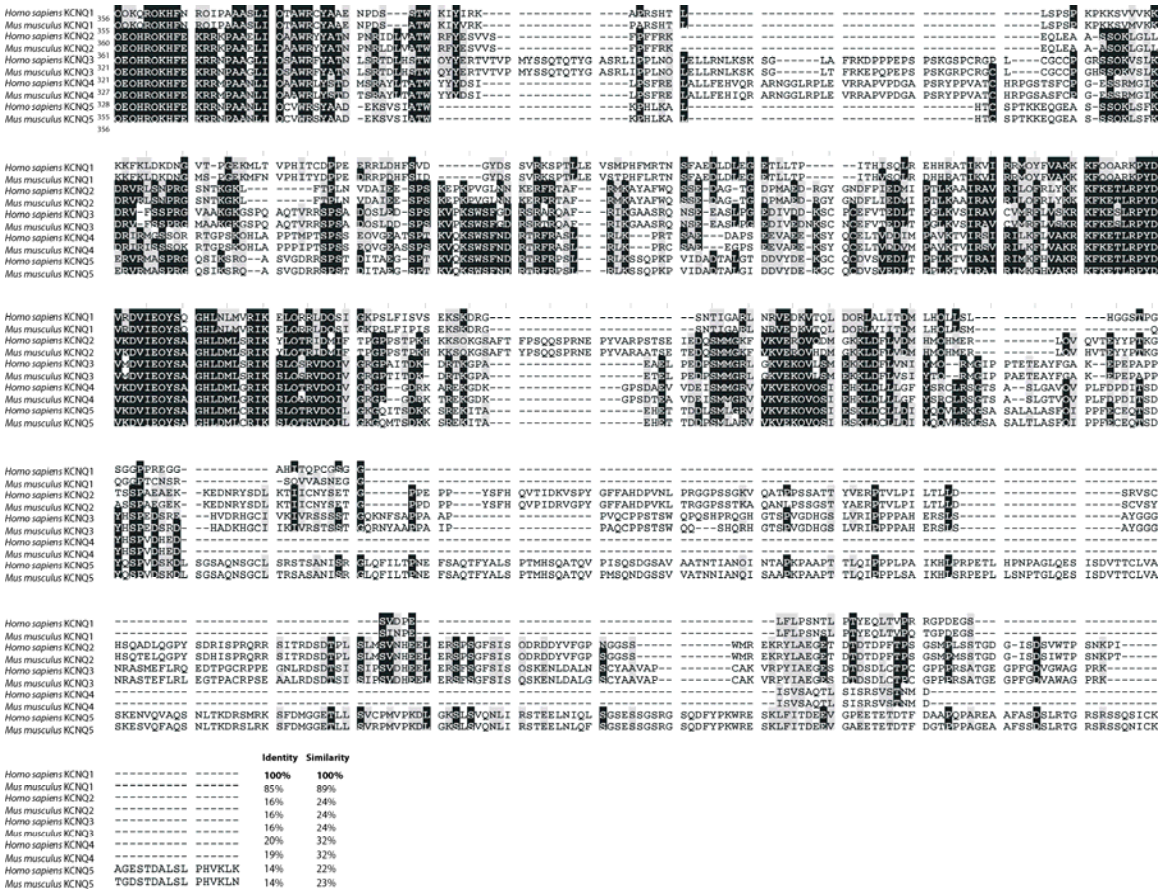

Figure S8: The C-terminus of KCNQ1 used to design antigenic epitopes is different from other members of the KCNQ channel family.

Multiple alignment of the C-terminal protein sequence of mouse and human KCNQ1 channels compared to the other mouse KCNQ protein family members. The black boxes indicate identical residues while grey boxes indicate residues with similar biochemical properties shared between channels. The percent similarity and percent identity of the C-terminus amino acid sequence compared to the human KCNQ1 protein were calculated using the Sequence Manipulation Suite Webserver (S11). Although full length protein sequences for both mouse and human KCNQ1-5 channels were used in the multiple alignment only the C-terminus is shown for comparative purposes. The multiple alignment was performed with the MUSCLE webserver (S9, S10).

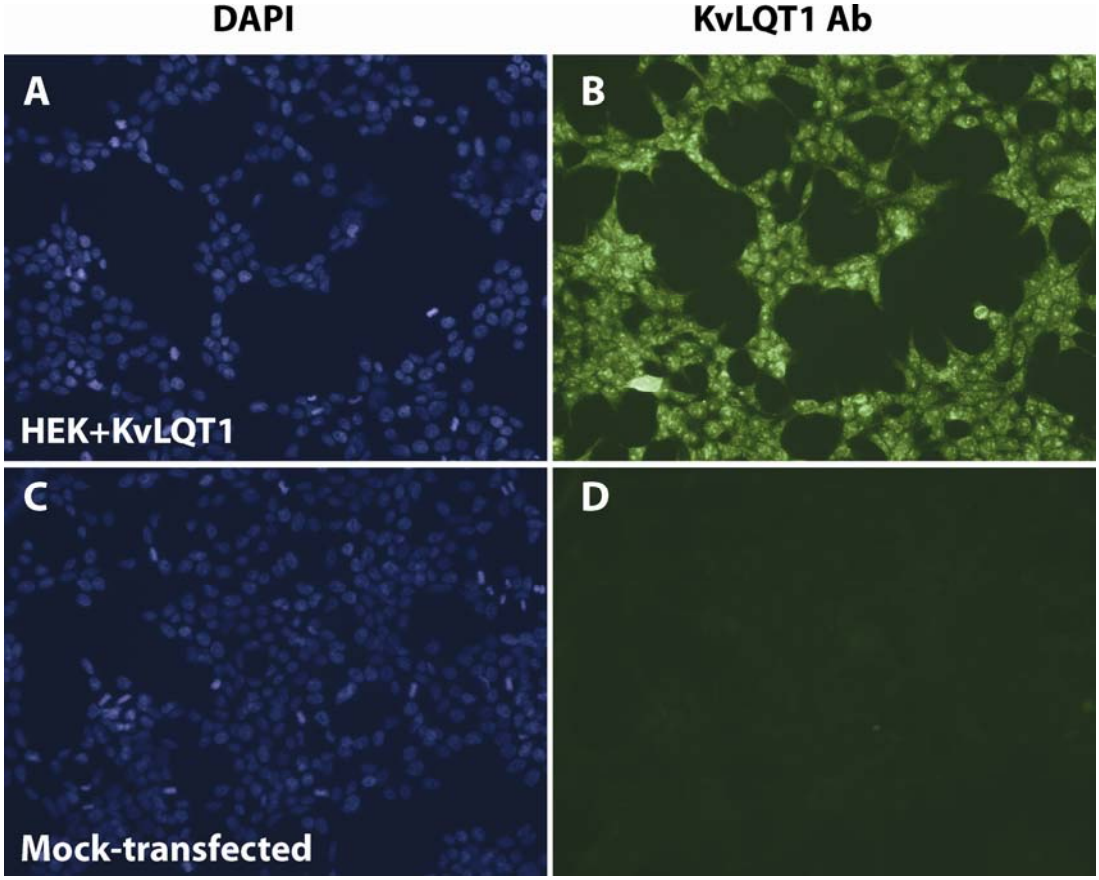

Figure S9: Immunocytochemical detection of mouse KvLQT1 protein expression in transiently-transfected HEK 293 cells. Immunospecific protein expression was detected following incubation with the polyclonal antibody to KvLQT1 in cells 24 hours post-transfection with cDNA encoding full length murine KvLQT1 (B), but not in cells that were mock-transfected (D). DAPI nuclear staining for the cells expressing KvLQT1 (A) and for those that were mocktransfected(C) are shown. HEK 293 cells were plated on glass coverslips in 35mm cell culture dishes and transfected with cDNA containing full length mouse *Kcnq1* (isoform 1) in pCMV-SPORT6, or mock-transfected (in the absence of cDNA), using FuGENE-6 (Boehringer Mannheim). Twenty-four hours posttransfection,the cells were processed using the same methodology as the brain IHC using anti-KvLQT1 (Millipore).

Supplemental References and Notes

S1. M.C. Sanguinetti, M.E Curran, A. Zou, J. Shen, P.S. Spector, D.L. Atkinson & M.T. Keating. Coassembly of K(V)LQT1 and minK (IsK) proteins to form cardiac I(Ks) potassium channel. *Nature* 384, 80-83 (1996).

S2. C. Chouabe, N. Neyroud, P. Guicheney, M. Lazdunski, G. Romey & J. Barhanin. Properties of KvLQT1 K+ channel mutations in Romano-Ward and Jervell and Lange-Nielsen inherited cardiac arrhythmias. *EMBOJ* **1**6, 5472-5479 (1997).

S3. M.P. Lee, R.J. Hu, L.A. Johnson & A.P. Feinberg. Human KVLQT1 gene shows tissue-specific imprinting and encompasses Beckwith-Wiedemann syndrome chromosomal rearrangements. *Nat. Gent.* 15, 181-185 (1997).

S4. S. Jiang, M.A. Hemann, M.P. Lee & A.P. Feinberg. Strain-dependent developmental relaxation of imprinting of an endogenous mouse gene, Kvlqt1. *Genomics* 53, 395-399 (1998).

S5. C. Kubisch, B.C. Schroeder, T. Friedrich, B. Lütjohann, A. El-Amraoui, S. Marlin, C. Petit & T.J. Jentsch. KCNQ4, a novel potassium channel expressed in sensory outer hair cells, is mutated in dominant deafness. *Cell* 96, 437-446 (1999).

S6. S. Demolombe, D.Franco, P. de Boer, S. Kuperschmidt, D. Roden, Y. Pereon, A. Jarry, A.F. Moorman & D. Escande. Differential expression of KvLQT1 and its regulator IsK in mouse epithelia. *Am. J. Physiol. - Cell Physiol.* 280, C359-72 (2001).

S7. X. Luo, J. Xiao, H. Lin, H., Y. Lu, B. Yang & Z. Wang. Genomic structure, transcriptional control, and tissue distribution of HERG1 and KCNQ1 genes. *Am. J. of Physiol. - Heart & Circ. Physiol.* 294, H1371-80 (2008).

S8. K. Tsuji, M. Akao, T.M. Ishii, S. Ohno, T. Makiyama, K. Takenaka, T. Doi, Y. Haruna, H. Yoshida, T. Nakashima, T. Kita, M. Horie. Mechanistic basis for the pathogenesis of long QT syndrome associated with a common splicing mutation in KCNQ1 gene. *J Mol Cell Cardiol .* 42, 662-669 (2007).

S9. R.C. Edgar. MUSCLE: a multiple sequence alignment method with reduced time and space complexity. *BMC Bioinfo.* 5, 113 (2004).

S10. R.C. Edgar. MUSCLE: multiple sequence alignment with high accuracy and high throughput. *Nucleic Acids Res.* 32, 1792-1797 (2004).

S11. P. Stothard. The Sequence Manipulation Suite: JavaScript programs for analyzing and formatting protein and DNA sequences. Biotechniques 28:1102-1104 (2000).